Electronic Supplementary Material (ESI) for Journal of Materials Chemistry C.

Electronic Supplementary Information

Trifunctional NiO–Ag–NiO Electrodes for ITO–Free Electrochromic Supercapacitors

Wenjie Dong,[ab] Ying Lv,[*a] Nan Zhang,[a] Lili Xiao,[ab] Yi Fan[a] and Xingyuan Liu[*a]

[a] *State Key Laboratory of Luminescence and Applications, Changchun Institute of Optics, Fine Mechanics and Physics, Chinese Academy of Sciences, Changchun 130033, China*

[b] *University of Chinese Academy of Sciences, Beijing 100049, China*

* Corresponding-Author, E-mail address: lvying@ciomp.ac.cn; liuxy@ciomp.ac.cn

Tel: +86-431-86176341

Content

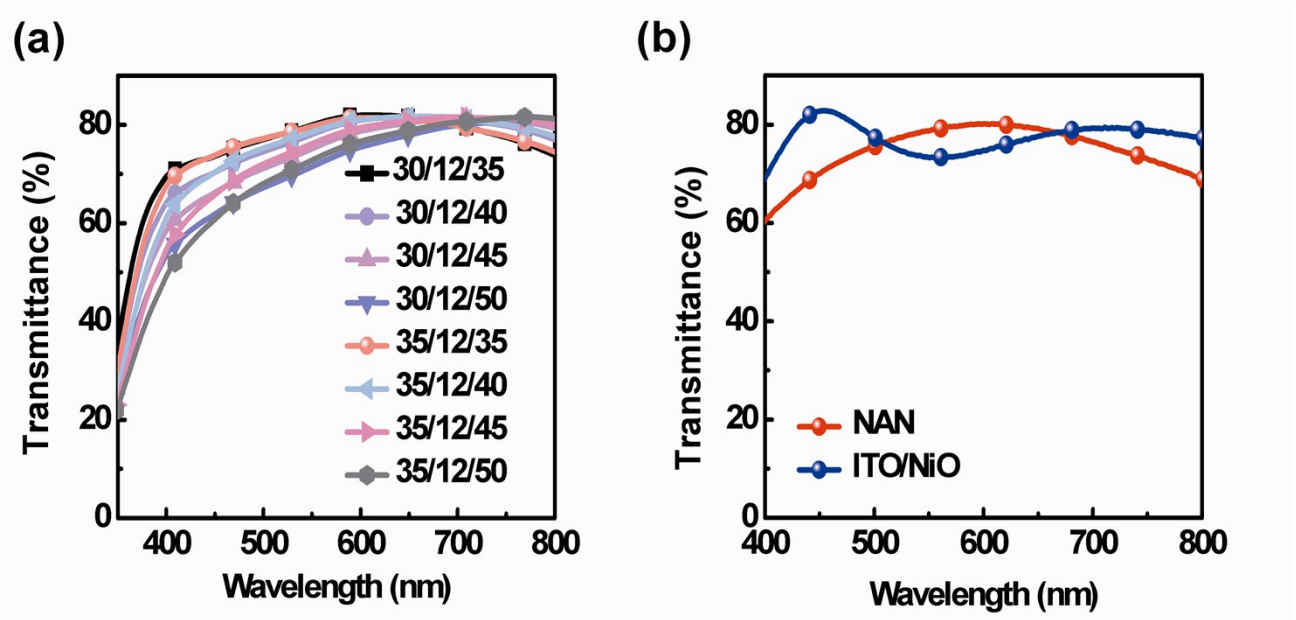

Figure S1. (a) Simulated transmittance spectra of NAN film with various NiO thickness; (b) Measured transmittance spectra of as-prepared NAN and ITO/NiO films.

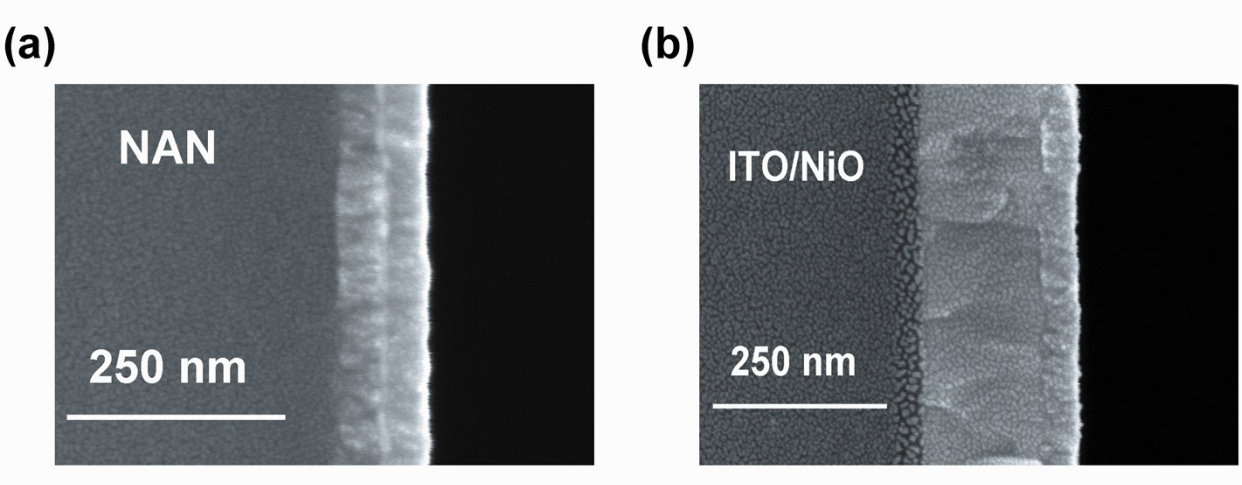

Figure S2. Cross sections SEM images of (a) NAN film deposited on glass substrate and (b) NiO film deposited on ITO substrate.

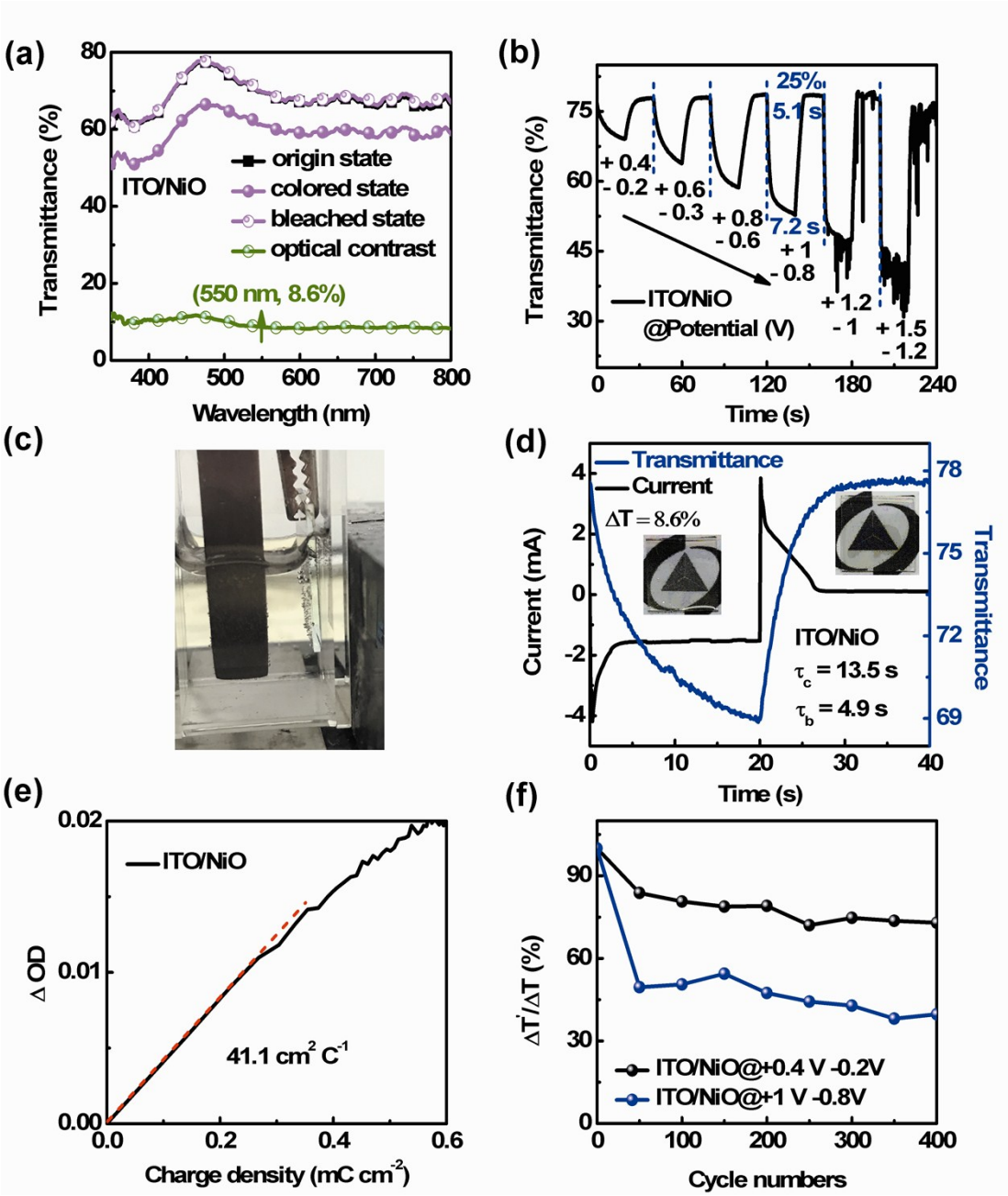

Figure S3. (a) Measured transmittance variation; (b) *in-situ* corresponding transmittance (550 nm) switching curves of ITO/NiO film at different potential; (c) picture taken at potential of +1.2/-1.0 V; (d) *in-situ* corresponding transmittance (550 nm) and chronoamperometry switching

curves (color changes presented in the inset) of NiO film on ITO substrate during potential stepping from +0.40 to –0.20 V (*vs.* Ag/AgCl) with a 20 s interval; (e) variation of the optical density (Δ*OD*, 550 nm) *vs.* charge density of NiO film on ITO substrate. (f) attenuation curves of optical contrast during 400 potential step cycles at different potential of ITO/NiO film.

When the potential was stepped between 0.4 to -0.2 V, the optical contrast of ITO/NiO film was only 8.6%, which is greatly lower than a value of 24.3% of NAN film. As shown in Figure S3b, the optical contrast exhibits a strong potential dependency. When the driving potential was increased to +1.0/–0.8 V, the optical contrast of ITO/NiO film at 550 nm was 25.1%, which is comparable with that of NAN film. Although larger optical contrast can be obtained if the potential was further increased. However, keep increasing potential to +1.2/–1.0 V can cause some decomposition of water to produce bubbles as shown in Figure S3c, which would cause the stripping of active materials from electrode and is contrary to the pursuit of high electrochemical stability. So, in ITO/NiO system, careful control of driving potential is very important to restrict the possible decrease of performance induced by eletrolyte.

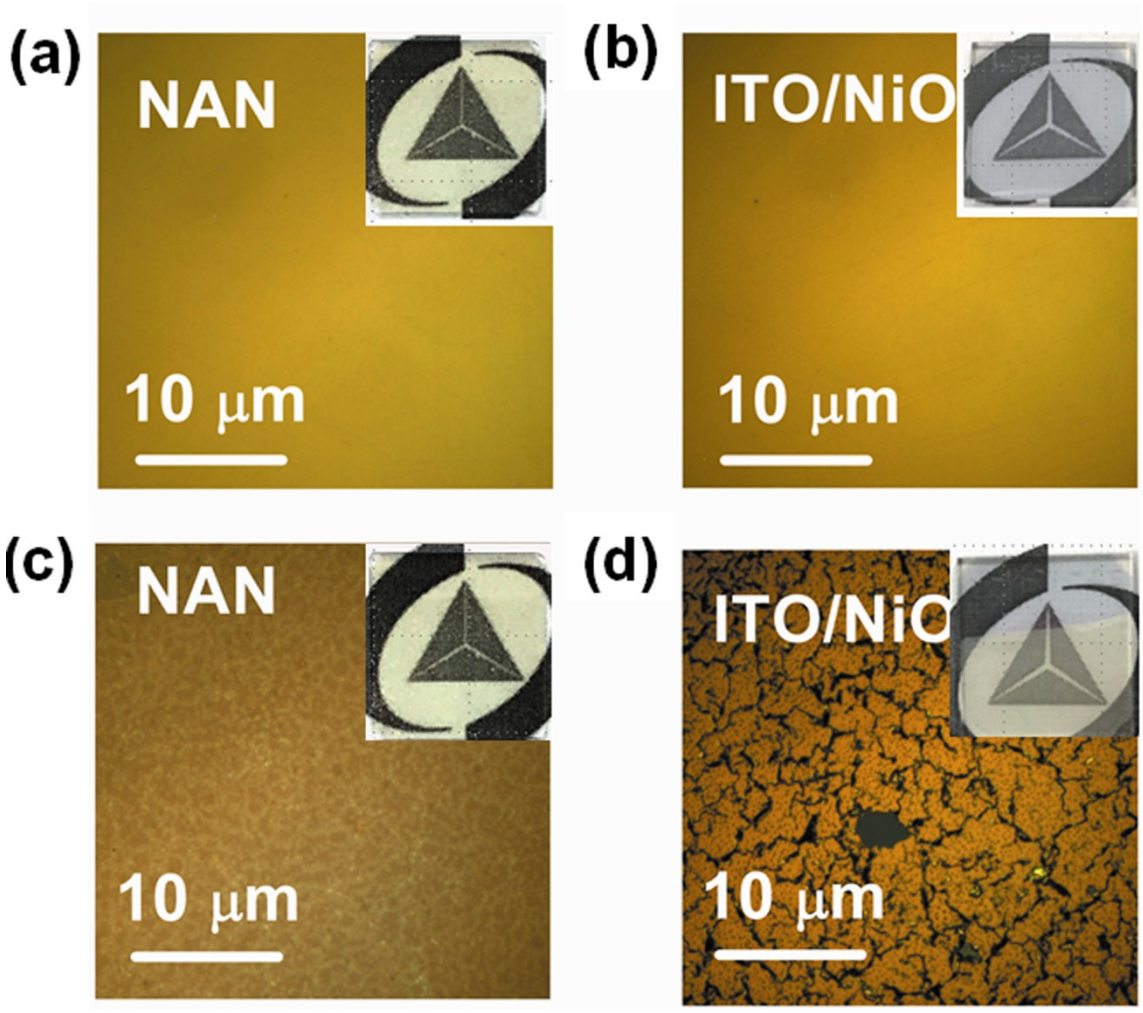

Figure S4. Optical microscope images of NAN and ITO/NiO films (a, b) before and (c, d) after electrochemical cycling for 400 times. The driving potential for NAN and ITO/NiO film are +0.4/-0.2 V and +1/-0.8 V, respectively. The insets are photographs of the films at each state.

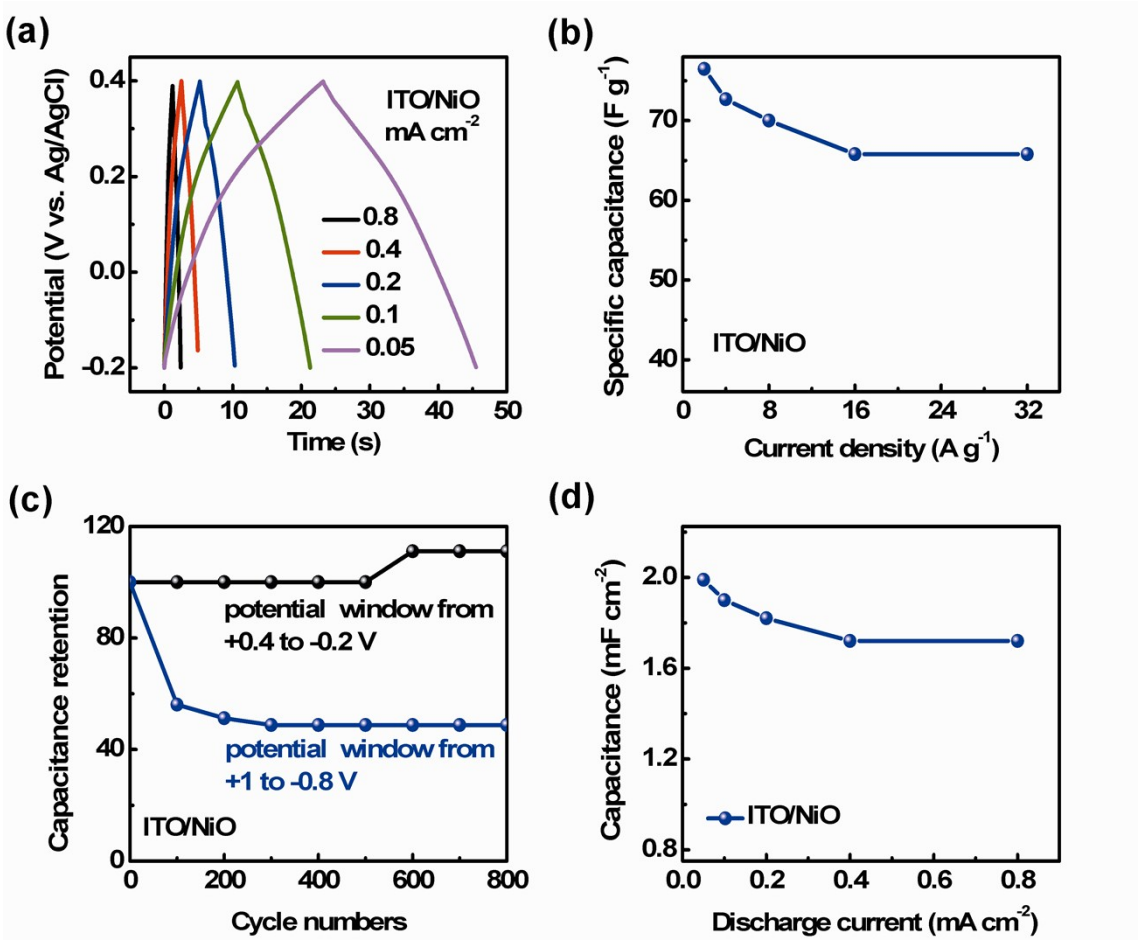

Figure S5. (a) Galvanostatic charging and discharging measurements of ITO/NiO film at different current density; (b) Calculated specific capacitance results of ITO/NiO film; (c) Long term cycling stability of ITO/NiO film after 800 cycles at a current density of 0.8 mA cm^{-2} at different potential window. The area capacitance increased to 111.1% of the initial value with potential window from +0.4 to -0.2 V. While for the potential window from +1 to -0.8 V, the capacitance retention decreased to 48.7% of the initial value；(d) Calculated area capacitance results of ITO/NiO film.

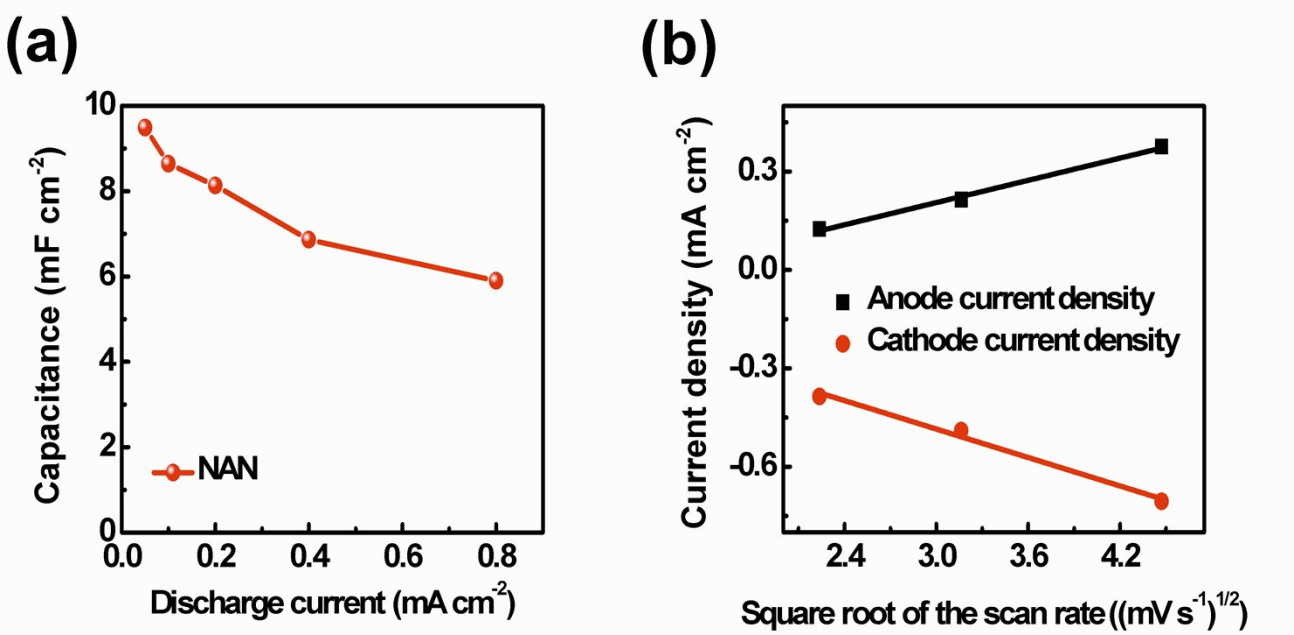

Figure S6. (a) Calculated area capacitance results of NAN film on glass substrate. (b) Peak current density of NAN film as a function of square root of scan rate $v^{1/2}$ of NAN film.

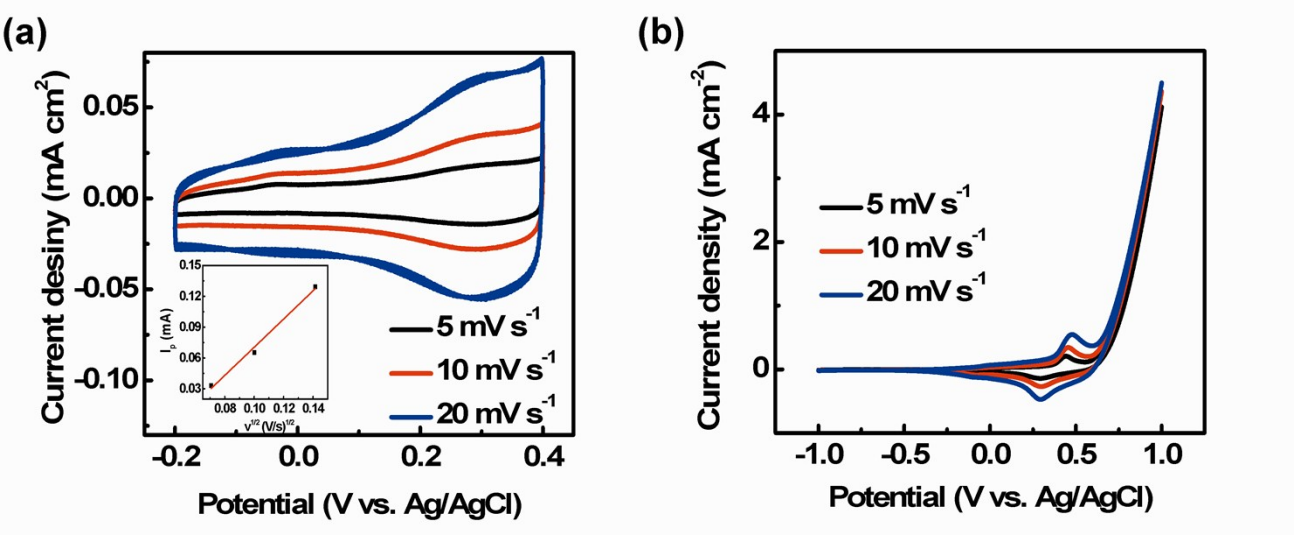

Figure S7. CV curves of ITO/NiO film on glass substrate at different scan speeds (a) at potential condition of +0.4/-0.2 V (peak current I_p as a function of square root of scan rate $v^{1/2}$ tested at room temperature in the inset); (b) at potential condition of +1/-1 V.

In Figure S7a, the CV cures of ITO/NiO films didn't show typical pair of redox peaks at the different scan rates from 5 to 20 mV s^{-1} and scan range from +0.4 to -0.2 V. But the typical pair of redox peaks appeared at the scan range of +1.0 to -1.0 V.

Table S1. Parameters measured by Hall effect measurement system.

Sample	Bulk carrier concentration (cm^{-3})	Mobility ($cm^2 \cdot V^{-1} \cdot s^{-1}$)	Resistivity ($\Omega \cdot cm$)	Sheet carrier concentration (cm^{-2})	*1Calculated square resistance (Ω $\square^{-1}$)	*2Measured square resistance (Ω $\square^{-1}$)
NAN-35	-1.617E+22	10.31	3.746E-5	-1.293E+17	8.0	9.6
NAN-50	-1.269E+22	9.794	5.022E-5	-1.244E+17	8.1	10.3

*1 Square resistance calculated by Hall measurement.

*2 Square resistance measured by four-point probe.

The sheet resistance of ITO, NAN-35 and NAN-50 films determined by four-point probe measurement are 11.0, 9.6 and 10.3 Ω $\square^{-1}$. The sheet resistance of NAN-35 and NAN-50 films was also determined by HMS-3000 Hall effect measurement system with an applied magnetic field of 0.55 T and calculated according to the following equation:

$$R = \rho / d$$

where R presents the sheet resistance, ρ denotes the resistivity and d is the thickness of Ag layer and the outer NiO. So, the calculated sheet resistance of NAN-35 and NAN-50 films are 7.97 and 8.10 Ω $\square^{-1}$, which were essentially in agreement with the results measured by four-point probe.

Table S2. Electrochromic performances summary of NAN and other selected nanostructured NiO films.

Structure	Synthesis method	*Temperature* (°C)	*Thickness of EC layer* (nm)	*Colored/bleached response time* (s)	*Coloration efficiency @Wavelength* (cm^2C^{-1}@nm)	Reference
Amorphous uniform NAN thin film	**Electron-beam deposition**	**room temperature**	**35**	**4.3/4.0**	**76.6@550**	**This study**
nanotubular NiO gyroid-structure	Electrode-deposition	450	460	0.063/0.053	47@630	**S1**
nanocrystalline NiO	fuel-assisted solution method	450	~200	11.8/4	25.8@550	**S2**
uniform NiO nanoparticles	solvothermal method	350	380	11.5/9.5	42.8@550	**S3**
nanoporous NiO	potentiostatically electrodeposition	300	229	N/A	54@630	**S4**
NiO nanosheets	template method	300	N/A	5.4/3.6	43.5@550	**S5**
hierarchical SnO_2@NiO core/shell nanoflake arrays	hydrothermal method + chemical bath deposition	400	350	1.7/2.4	43.5@550	**S6**
ordered porous NiO	template-assisted electrodeposition	300	~250	3/6	41.1@550	**S7**
Co-doped NiO nanoflake array	chemical bath deposition	350	~250	3.4/5.4	47.7@550	**S8**
NiO nanorodes	HFMOVD	1200	500	1.55/1.22	43.3@550	**S9**
nanoscale NiO grains	Aerosol-assisted chemical vapor deposition	450	N/A	4.1/3.6	45@550	**S10**

REFERENCES

S1 M. R. J. Scherer and U. Steiner, *Nano Lett.,* 2013, **13**, 3005-3010.

S2 K. K. Chiang and J.J. Wu, *ACS Appl. Mater. Interfaces,* 2013**, 5**, 6502-6507.

S3 G. Cai, X. Wang, M. Cui, P. Darmawan, J. Wang, A. L. S. Eh and Lee. P. S, *Nano Energy,* 2015**,** 12, 258-267.

S4 D. S. Dalavi, M. J. Suryavanshi, S. S. Mali, D. S. Patil and P. S. Patil, *J. Solid State lectrochem.*, 2012, **16**, 253-263.

S5 C. Zhao, C. Chen, F. Du and J. Wang, *RSC Adv.*, 2015, **5**, 38533-38537.

S6 J.-h. Zhang, J.-p. Tu, D. Zhou, H. Tang, L. Li, X.-l. Wang and C.-d. Gu, *J. Mater. Chem. C*, 2014, **2**, 10409-10417.

S7 Y. F. Yuan, X. H. Xia, J. B. Wu, Y. B. Chen, J. L. Yang and S. Y. Guo, *Electrochim. Acta*, 2011, **56**, 1208-1212.

S8 J. Zhang, G. Cai, D. Zhou, H. Tang, X. Wang, C. Gu and J. Tu, *J. Mater. Chem. C*, 2014, **2**, 7013-7021.

S9 R. A. Patil, R. S. Devan, J.-H. Lin, Y.-R. Ma, P. S. Patil and Y. Liou, *Sol. Energy Mater. Sol. Cells*, 2013, **112**, 91-96.

S10 M. Z. Sialvi, R. J. Mortimer, G. D. Wilcox, A. M. Teridi, T. S. Varley, K. G. U. Wijayantha and C. A. Kirk, *ACS Appl. Mater. Interfaces*, 2013, **5**, 5675-5682.